RefDrone: A Challenging Benchmark for Referring Expression Comprehension in Drone Scenes

Zhichao Sun[1] **Yepeng Liu**[1] **Huachao Zhu**[1] **Yuliang Gu**[1] **Yuda Zou**[1]
Zelong Liu[1] **Gui-Song Xia**[1] **Bo Du**[1] **Yongchao Xu**[1]*
[1]School of Computer Science, Wuhan University

Abstract

Drones have become prevalent robotic platforms with significant potential in Embodied AI. A crucial capability for drone-based Embodied AI is Referring Expression Comprehension (REC), which enables locating objects with language expressions. Despite advances in REC for ground-level scenes, drones' unique capability for broad observation introduces distinct challenges: multiple potential targets, small-scale objects, and complex environmental contexts. To address these challenges, we introduce RefDrone, an REC benchmark for drone scenes. RefDrone reveals three key challenges: 1) multi-target and no-target scenarios; 2) multi-scale and small-scale target detection; 3) complex environment with rich contextual reasoning. To efficiently construct this dataset, we develop RDAnnotator, a semi-automated annotation framework where specialized modules and human annotator collaborate through feedback loops. RDAnnotator ensures high-quality contextual expressions while reducing annotation costs. Furthermore, we propose Number GroundingDINO (NGDINO), a novel method to handle multi-target and no-target cases. NGDINO explicitly estimates the number of objects referred to in the expression and incorporates this numerical pattern into the detection process. Comprehensive experiments with state-of-the-art REC methods demonstrate that NGDINO achieves superior performance on RefDrone, as well as on the general-domain gRefCOCO and remote sensing RSVG benchmarks. The data and code are completely available at https://github.com/sunzc-sunny/refdrone.

1 Introduction

Drones/UAVs have become increasingly popular in our daily lives, serving both personal and professional purposes, such as entertainment, package delivery, traffic surveillance, and emergency rescue [1, 42, 45]. Their ability to move freely and to observe broadly make them important platforms for Embodied AI applications [12, 35, 23, 14, 31]. A crucial capability in Embodied AI is Referring Expression Comprehension (REC) [43, 48, 4, 49], which serves as a critical bridge between natural language understanding and visual perception. REC requires drones to localize specific objects in images based on natural language expressions. However, existing REC datasets primarily focus on ground-level perspectives, such as RefCOCO [54, 36] dataset. The application of REC in drone-based scenarios presents unique challenges.

In this work, we introduce **RefDrone**, a challenging REC benchmark for drone scenes. RefDrone comprises 17,900 referring expressions annotated over 8,536 images, with 63,679 object instances. As illustrated in Figure 1, RefDrone poses three primary challenges that distinguish it from existing datasets: (1) **multi-target and no-target samples**, where expressions may refer to any number of objects, ranging from 0 to 242; (2) **multi-scale and small-scale target detection**, with 31% small

*Corresponding author.

Preprint. Under review.

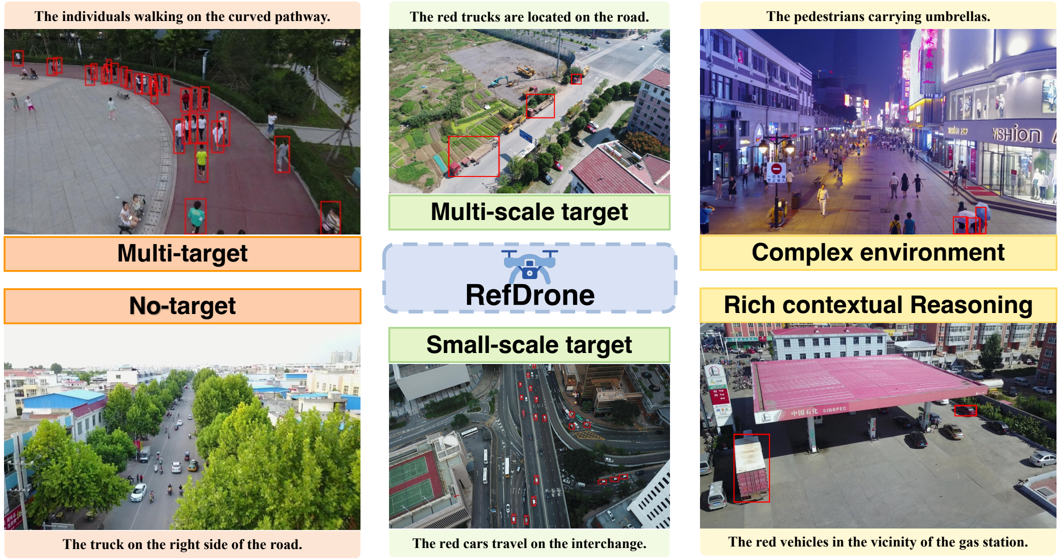
The individuals walking on the curved pathway.
Multi-target
The red trucks are located on the road.
Multi-scale target
The pedestrians carrying umbrellas.
Complex environment
RefDrone
No-target
Small-scale target
Rich contextual Reasoning
The truck on the right side of the road.
The red cars travel on the interchange.
The red vehicles in the vicinity of the gas station.

Figure 1: Examples of the various challenges in RefDrone dataset.

objects and 14% large objects; and (3) **complex environment with rich contextual reasoning**, encompassing diverse viewpoints, lighting conditions, and intricate backgrounds. The referring expressions richly capture spatial relations, object attributes, and inter-object interactions. As summarized in Table 1, RefDrone offers greater diversity and complexity than previous REC benchmarks. We further evaluate **13 representative REC models** using both fine-tuning and zero-shot settings. Notably, all models exhibit significantly poorer performance on RefDrone compared to standard REC datasets (*e.g.*, *GroundingDINO [34] yields 21.07* $Acc_{img.}$ *on RefDrone vs. 91.4* $Acc_{img.}$ *on RefCOCO*), highlighting the inherent difficulty and unique challenges posed by our benchmark.

To efficiently construct RefDrone, we develop RDAnnotator, a semi-automated annotation pipeline for referring expression annotation in drone scenes. RDAnnotator leverages multiple specialized LMM-based modules, which collaborate within a feedback loop to generate and validate annotations. This tool reduces human involvement to quality control and minor adjustments, thereby significantly lowering annotation costs, while maintaining high-quality standards for complex expressions. RDAnnotator achieves a cost of just **$0.0539 per expression** (GPT-4o API usage) and reduces human annotation time to under **one minute per expression**. This cost-efficiency makes RDAnnotator a scalable solution for large-scale dataset construction and can be readily adapted to other REC tasks.

Furthermore, we propose Number GroundingDINO (NGDINO) to address the challenges of multi-target and no-target referring expressions. Our key insight is that ***explicitly utilizing the number information of referred objects enhances the handling of these scenarios***. NGDINO includes three key components: (1) a number prediction head that estimates the count of target objects, (2) learnable number-queries that capture numerical patterns corresponding to varying object quantities, and (3) a number cross-attention module that fuses number queries with detection queries to inform object localization. Extensive experiments on both our RefDrone benchmark, as well as the general-domain gRefCOCO [28] and remote sensing RSVG [56] datasets, demonstrate that NGDINO substantially improves performance, particularly in the challenging multi-target and no-target cases.

In summary, our contributions are listed as follows:

- **RefDrone Benchmark**: We introduce RefDrone, a comprehensive benchmark for referring expression comprehension in drone scenes. RefDrone poses three key challenges: multi-target/no-target scenarios, multi-scale/small-object detection, and complex contextual reasoning. We provide thorough baseline evaluations with 13 representative REC models.
- **RDAnnotator Framework**: We propose RDAnnotator, a semi-automated annotation framework that significantly reduces human effort while ensuring high-quality referring expressions. This framework is scalable for large-scale dataset construction and generalizable beyond drone imagery.
- **NGDINO Method**: We develop NGDINO, a novel approach that explicitly models the number of referred objects to address multi-target and no-target cases. NGDINO achieves

state-of-the-art performance on RefDrone and shows consistent improvements on gRefCOCO and RSVG benchmarks.

Table 1: Comparison of REC datasets relevant to RefDrone. Avg. objects: mean objects per expression. Avg. length: mean words per expression. No target: expressions without referred objects. Expression type: method for expression generation. Small target: percentage of small-scale objects.

	RefCOCO/+/g [54, 36]	gRefCOCO [28]	D^3 [51]	RIS-CQ [19]	RSVG [56]	RefDrone (Ours)
Image source	COCO [26]	COCO [26]	COCO [26]	VG [22]+COCO [26]	DIOR [24]	VisDrone [60]
Avg. objects	1.0	1.4	1.3	3.6	2.2	3.8
Avg. length	3.6/3.5/8.4	4.9	6.3	13.2	7.5	9.0
No target	✗	✓	✓	✗	✗	✓
Expression type	Manual	Manual	Manual	LLM (GPT3.5-t)	Templated	LMM (GPT4-o)
Small target	0/0/0%	0.1%	6.3%	-	17.2%	31.1%

2 Related Works

2.1 Referring expression understanding datasets

Referring expression understanding identifies regions in visual content from natural language expressions. The main subtasks are Referring Expression Comprehension (REC), which outputs detection bounding boxes, and Referring Expression Segmentation (RES), which outputs segmentation masks. Datasets in this domain show increasing visual and linguistic complexity. Early datasets such as ReferIt [21] and RefCOCO [54] are pioneering but limited to simple expressions and single-target scenarios. Later datasets [32, 9, 28, 46, 19, 51] introduce more challenges. gRefCOCO [28] supports multi-target expressions. OV-VG [46] enables open-vocabulary queries. D^3 [51] and RIS-CQ [19] offer more complex expressions. Domain-specific datasets [10, 8, 56, 37, 39] address specialized applications: RSVG [56] for remote sensing, RAVAR [37] for video action recognition, RIO [39] for affordance detection. However, drone scenes remain unexplored in REC, motivating our RefDrone benchmark. Table 1 compares RefDrone with other related REC benchmarks.

Recent dataset creation approaches leverage large language models (LLMs) to reduce annotation costs. Works such as LLaVA [30] and Ferret [53] demonstrate the effectiveness of LLMs in generating instruction tuning data. Similarly, RIS-CQ [19] and RIO [39] employ LLMs to generate referring expressions. However, these approaches treat LLMs as text generators and may lack proper visual grounding. In contrast, we employ a semi-automated annotation framework with iterative feedback mechanisms throughout the annotation pipeline to reduce annotation costs and improve quality.

2.2 Referring expression comprehension methods

REC methods can be broadly categorized into large multimodal models (LMMs) and specialist models. Large Multimodal Models [30, 53, 5, 7, 3, 38, 47, 27, 57, 50] have recently been applied to REC tasks as part of evaluating their broader visual-language understanding capabilities. These models leverage extensive referring instruction tuning data to achieve competitive performance without task-specific architectural designs. Despite their broad capabilities, LMMs consistently struggle with small object detection, primarily due to their inherent input resolution constraints. This constraint forces image downsampling, resulting in the loss of fine-grained visual details.

Specialist models include two-stage and one-stage methods. Two-stage methods [18, 29, 16, 44, 15] typically approach REC as a ranking task: first generating region proposals through a detector, then ranking them based on their alignment with the language input. However, they are often criticized for slow inference speeds. In contrast, one-stage methods [20, 25, 33, 13, 52, 34] directly predict target regions guided by language input. These approaches leverage transformer to enable cross-modal interactions between visual and textual features. Among these methods, GroundingDINO (GDINO) [34] has gained widespread attention for its impressive results in REC tasks. Our work extends GDINO by incorporating explicit number modeling to handle multi-target and no-target scenarios, which are critical challenges in drone-based REC tasks.

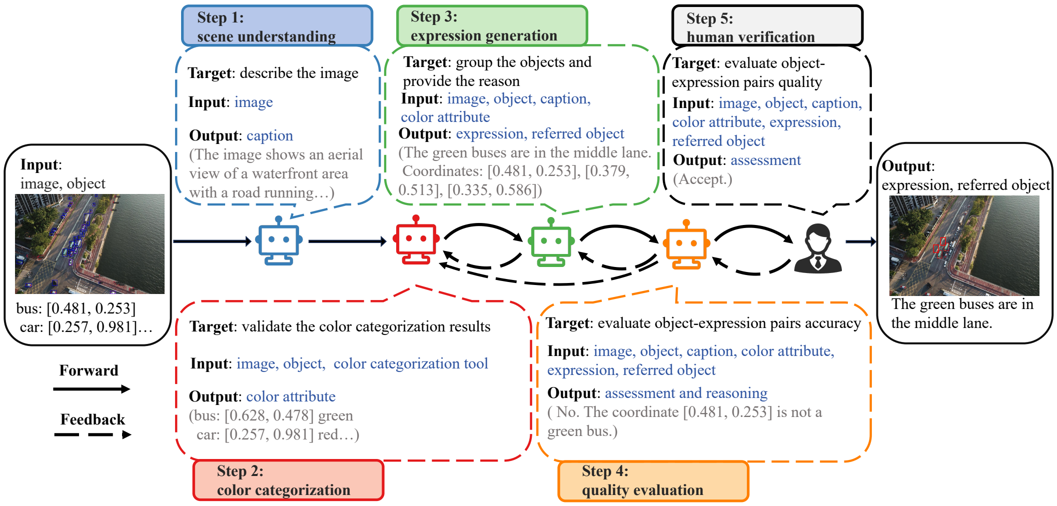
Step 1:
scene understanding
Target: describe the image
Input: image
Output: caption
(The image shows an aerial view of a waterfront area with a road running…)
Step 3:
expression generation
Target: group the objects and provide the reason
Input: image, object, caption, color attribute
Output: expression, referred object
(The green buses are in the middle lane.
Coordinates: [0.481, 0.253], [0.379, 0.513], [0.335, 0.586])
Step 5:
human verification
Target: evaluate object-expression pairs quality
Input: image, object, caption, color attribute, expression, referred object
Output: assessment
(Accept.)
Input:
image, object
bus: [0.481, 0.253]
car: [0.257, 0.981]…
Output:
expression, referred object
The green buses are in the middle lane.
Forward
Feedback
Target: validate the color categorization results
Input: image, object, color categorization tool
Output: color attribute
(bus: [0.628, 0.478] green
car: [0.257, 0.981] red…)
Step 2:
color categorization
Target: evaluate object-expression pairs accuracy
Input: image, object, caption, color attribute, expression, referred object
Output: assessment and reasoning
(No. The coordinate [0.481, 0.253] is not a green bus.)
Step 4:
quality evaluation

Figure 2: The overview of the RefDrone annotation process with RDAnnotator. Multiple specialized LMM-based modules collaborate both with each other and human annotators through iterative feedback loops to generate high-quality annotations.

3 RefDrone benchmark

3.1 Data source

The RefDrone benchmark is built upon VisDrone2019-DET [60], a large-scale high-quality drone-captured object detection dataset. Source images are collected across multiple scenarios, illumination conditions, and flying altitudes. To ensure meaningful visual content, we filter out images with fewer than three objects and objects with bounding box areas below 64 pixels. VisDrone2019-DET provides object categories and bounding box coordinates, which we convert to normalized center points (range 0-1). This approach reduces the input context for LMMs while preserving spatial information.

3.2 RDAnnotator for semi-automated annotation

RDAnnotator (referring drone annotator) is a semi-automated annotation framework that minimizes human effort while ensuring high quality. It integrates specialized modules powered by LMMs with human validation. As shown in Figure 2, RDAnnotator employs five structured steps.

Step 1: scene understanding. A GPT-4o-based scene parsing module generates three diverse textual descriptions per image. These captions establish spatial layouts, object relationships, and contextual foundations to guide subsequent referring expression generation.

Step 2: color categorization. Color attributes are crucial discriminative features in referring expressions. We implement a hybrid color extraction pipeline, which combines low-level CNN-based classification (WideResNet-101 classifier [55]) with high-level LMM semantic reasoning, ensuring robust color attribution in challenging aerial conditions.

Step 3: expression generation. To address the complexity of referring expression generation, we reformulate the referring expression generation task as an *object grouping problem*. The target of the module is to group semantically related objects and provide appropriate reasons for each group. The reasons serve as the referring expressions. Furthermore, a dynamic feedback loop triggers Step 2 (color categorization) when unseen colors are detected, ensuring color attribute consistency.

Step 4: quality evaluation. A validation module assesses the semantic accuracy and uniqueness of each object-expression pair, classifying each annotation as either correct (accurately and uniquely identifying the described objects) or incorrect (inaccurate or ambiguous, with an explanation of the identified issue). Annotations deemed correct proceed to Step 5 (human verification), while incorrect annotations trigger targeted feedback: those with semantic errors are returned to Step 3 (expression generation), and color-related inaccuracies are redirected to Step 2 (color categorization).

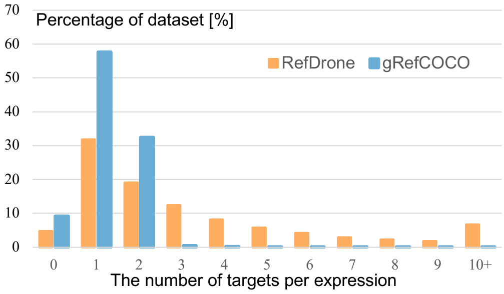

Figure 3: Object number distribution per expression in gRefCOCO [28] and RefDrone datasets.

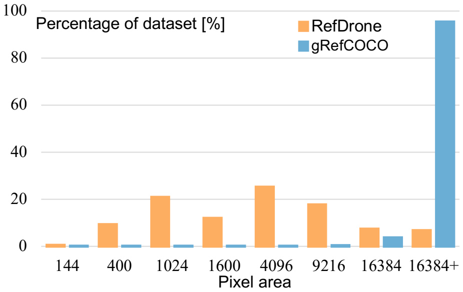

Figure 4: Object size distribution histograms in RefDrone and gRefCOCO [28] datasets.

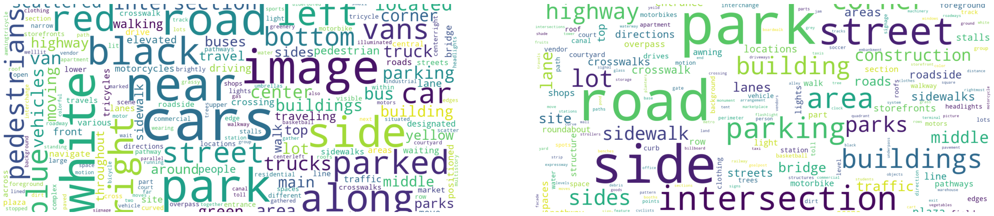

(a) Word cloud of complete expression.

(b) Word cloud of background terms.

Figure 5: Word frequency visualization in RefDrone dataset.

Step 5: human verification. Human annotators review annotation outputs in three tiers:

- *Direct acceptance*. Annotations satisfying all criteria are approved for the final dataset.
- *Refinement required*. Minor errors are corrected through human editing.
- *Significant issues*. Poorly grounded or inconsistent annotations trigger full regeneration.

Annotations with significant issues re-enter the pipeline at Step 4 (quality evaluation). If an annotation repeatedly fails, it is classified as a no-target sample. These feedback loops ensure all annotations meet quality standards and that no-target expressions are contextually relevant to the image.

Each step utilizes LMMs through in-context learning with carefully designed task-specific prompts and examples (see Appendix A.8). The final annotation quality demonstrates 42% directly accepted samples, 47% requiring minor refinement, and 11% demanding full re-annotation. RDAnnotator reduces human annotation effort by 85%, decreasing annotation time from 7 to 1 minute per expression, while incurring only $0.0539 per expression in GPT-4o API costs. This cost-performance balance makes the framework scalable for large-scale dataset creation while maintaining annotation quality.

3.3 Dataset analysis

The RefDrone dataset contains 17,900 referring expressions across 8,536 images, comprising 63,679 object instances in 10 categories. We retain the original train, validation, and test splits from VisDrone2019-DET [60]. The average expression length is 9.0 words, and each expression refers to an average of 3.8 objects. Figure 1 highlights the three key challenges in RefDrone:

1) Multi-target and no-target samples. Unlike conventional REC datasets [54, 36] that primarily focus on single-object references, RefDrone includes 11,362 multi-target and 847 no-target expressions. The number of referred targets per expression ranges from 0 to 242. Figure 3 illustrates the target number distribution, revealing higher complexity in multi-target scenarios compared to gRefCOCO, where the majority of expressions contain references to only one or two objects.

2) Multi-scale and small-scale target detection. Figure 4 presents the challenges of scale distribution: small-scale objects ($< 32^2$ pixels) make up 31% of instances, normal-scale (32^2-96^2 pixels) 55%, and large-scale ($> 96^2$ pixels) 14%. Compared to gRefCOCO [28], RefDrone has a notably higher variance in object scales, emphasizing the dataset's multi-scale challenges.

3) Complex environment with rich contextual reasoning. The images present inherent complexity, including diverse viewpoints, varying lighting conditions, and complex background environments. The referring expressions go beyond simple object attributes (*e.g.*, color, category) and spatial relationships (*e.g.*, 'left', 'near'), incorporating rich object-object interactions (*e.g.*, 'the white trucks carrying livestock') and object-environment interactions (*e.g.*, 'the white cars line up at the intersection'). Figure 5 visualizes this linguistic richness through word clouds of (a) complete expressions and (b) background terms, highlighting the diverse vocabulary used in descriptions.

3.4 Dataset comparison

Table 1 compares RefDrone with existing REC datasets. RefDrone stands out for its higher average number of referred objects and use of LMM for expression generation. Its expressions offer richer contextual details than template-based or human-annotated expressions [59]. While RIS-CQ [19] uses LLM for expression generation, it lacks visual content, often producing linguistically complex but visually disconnected expressions. Similarly, RSVG [56] focuses on small targets but lacks expression quality. In contrast, RefDrone comprehensively presents three challenges, establishing it as a challenging benchmark in REC tasks.

3.5 Evaluation metrics

We introduce instance-level metrics extending traditional REC metrics to address multi-target challenges. Previous benchmarks primarily focus on image-level metrics, which are sufficient for single-target or few-target samples. However, these metrics fail to handle expressions referring to multiple target objects—potentially scaling up to hundreds of instances per expression in our task. To address this limitation, these new metrics provide a more granular evaluation of a model's capability to identify individual target objects.

Instance-level metrics: Acc$_{inst.}$ and F1$_{inst.}$ provide a fine-grained evaluation of the ability to precisely localize individual target objects. We compute the intersection over union (IoU) between the true bounding boxes and the predicted bounding boxes. An IoU $\geq$ 0.5 is considered a true positive (TP), otherwise it is a false positive (FP). Unmatched true bounding boxes are counted as false negatives (FN). For no-target samples, a prediction without any bounding box is a true negative (TN), otherwise it is a false positive (FP). We calculate:

$$\text{Acc}_{inst.} = \frac{\text{TP} + \text{TN}}{\text{TP} + \text{TN} + \text{FP} + \text{FN}}, \quad (1) \qquad \text{F1}_{inst.} = \frac{2 \cdot \text{TP}}{2 \cdot \text{TP} + \text{FP} + \text{FN}}. \quad (2)$$

Image-level metrics: Acc$_{img.}$ and F1$_{img.}$ evaluate the overall accuracy at the image level. An expression is a true positive (TP) only if all predictions exactly match the true bounding boxes. Any partial or extra prediction is a false positive (FP). For no-target samples, no prediction is counted as a true negative (TN), otherwise a false positive (FP). Image-level metrics use the same formulations as instance-level metrics but are applied to whole expressions rather than individual objects.

4 NGDINO

We introduce Number GroundingDINO (NGDINO) to address multi-target and no-target challenges in REC. Our key insight is that explicit numerical reasoning about target counts enhances model performance on these challenges. NGDINO builds upon GDINO [34] while introducing three components: (1) a number prediction head, (2) learnable number-queries with number-guided query selection, and (3) a number cross-attention module.

NGDINO adopts GDINO's dual-encoder-single-decoder architecture. The image encoder extracts visual features from input images, while the text encoder processes referring expressions. A feature enhancer facilitates cross-modal fusion, and a language-guided query selection module initializes detection queries. The decoder iteratively refines detection queries through self-attention, image cross-attention, and text cross-attention mechanisms, ultimately producing bounding box predictions. We mainly improve the decoder part, as highlighted by the yellow box in Figure 6.

Number prediction head. We introduce a classification module to predict the number of referred objects N_{pred}. This prediction head consists of an FFN layer applied to the detection queries Q_{det}, followed by mean pooling:

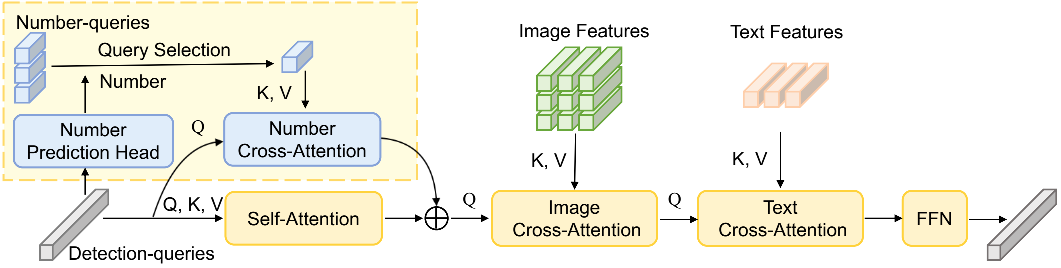

Figure 6: Architecture of a single decoder layer in Number GroundingDINO. Key modifications from GDINO [34] (highlighted in yellow box) include: (1) number prediction head (FFN) to predict target number, (2) number-queries selected through the predicted number, (3) number cross-attention between selected number-queries and detection-queries.

$$N_{prob} = \text{softmax}\ (\ \text{MeanPool}\ (\ \text{FFN}\ (Q_{det}))), \quad (3) \qquad N_{pred} = \text{argmax}\ (N_{prob}), \quad (4)$$

where $Q_{det} \in \mathbb{R}^{B \times L_d \times D}$ with batch size B, detection query length L_d, and feature dimension D. Rather than directly predicting arbitrary counts, we quantize the prediction space into five categories $\mathcal{C} = \{0, 1, 2, 3, 4+\}$, where $4+$ represents four or more targets. This quantization addresses the long-tailed distribution of target counts in real-world data (which follows Zipfian distribution [2]).

Number-queries and number-guided query selection. We introduce a learnable set of number-queries $Q_{num} \in \mathbb{R}^{B \times L_n \times D}$, where L_n is the length of number-queries. Q_{num} is randomly initialized and trained to capture numerical patterns. Based on the predicted target number N_{pred}, we select a subset of number-queries Q_{num}^{sel}:

$$Q_{num}^{sel} = Q_{num}\big[\ :,\ L_s \cdot N_{pred}\ :\ L_s \cdot (N_{pred} + 1),\ :\ \big], \quad (5)$$

where L_s is the length of selected number-queries. This creates a direct mapping between the predicted number of objects and the specialized queries that encode patterns relevant to that cardinality.

Number cross-attention module. We integrate the number information into the object detection process through a number cross-attention mechanism that operates in parallel with the self-attention in the decoder. In number cross-attention, detection queries Q_{det} serve as queries (Q), while the selected number-queries Q_{num}^{sel} serve as both keys (K) and values (V). The output of this module is added to the self-attention features before subsequent processing in the decoder layer.

Training objective. We adopt GDINO's bounding box supervision and add a Cross-Entropy loss for number prediction. Ablation studies determine the optimal parameters: selected number-query length $L_s = 10$ and total number-query length $L_n = 50$, matching our 5-category quantization scheme.

5 Experiments

We establish the benchmark with 13 representative models that can perform REC tasks, comprising 3 specialist models and 10 LMMs. The specialist models include MDETR [20], GLIP [25], and GDINO [34]. For the LMMs, we evaluate Shikra [7], ONE-PEACE [47], SPHINX-v2 [27], MiniGPT-v2 [5], Ferret [53], Kosmos-2 [38], Griffon [57], Qwen-VL [3], CogVLM [50], and LLaVA [30]. Detailed model specifications and implementation details are provided in the Appendix.

5.1 Experimental results

Fine-tuning results. Table 2 illustrates fine-tuning performance across multiple methods on our RefDrone dataset. The consistently poor performance across all approaches highlights the inherent challenges of the proposed dataset. The specialist model MDETR [20] shows strong performance in instance-level metrics, achieving comparable results to GDINO-B [34], but struggles with image-level understanding. Conversely, LMMs like Qwen-VL [3] achieve superior image-level comprehension while struggling with instance-level tasks. This performance disparity can be attributed to LMMs' effective global image understanding capabilities but limited effectiveness in detecting small objects due to input resolution constraints (detailed results by object scale are provided in Appendix Table 9).

Table 2: Experimental results of fine-tuning baselines on RefDrone benchmark. Top groups: specialist models. Bottom groups: LMMs for REC tasks. GDINO-T and GDINO-B denote GroundingDINO [34] with Swin-Tiny and Swin-Base backbones. The best results in each group are denoted with **bold**.

Methods	F1$_{inst.}$	Acc$_{inst.}$	F1$_{img.}$	Acc$_{img.}$
MDETR [20]	32.60	19.49	19.17	10.81
GLIP [25]	24.23	14.86	16.92	13.29
GDINO-T [34]	30.50	19.02	29.65	21.07
NGDINO-T (Ours)	33.34	20.98	32.45	22.84
GDINO-B [34]	31.96	19.99	31.69	22.26
NGDINO-B (Ours)	**34.44**	**21.76**	**34.01**	**23.89**
MiniGPT-v2 [5]	4.97	2.74	13.56	8.97
LLaVA-v1.5 [30]	6.00	3.63	14.43	**11.57**
Qwen-VL [3]	**14.14**	**7.61**	**20.10**	11.17

Table 3: Experimental results of zero-shot baselines on RefDrone benchmark. Top groups: specialist models. Bottom groups: LMMs for REC tasks.

Methods	F1$_{inst.}$	Acc$_{inst.}$	F1$_{img.}$	Acc$_{img.}$
MDETR [20]	**8.42**	**4.41**	2.99	1.63
GLIP [25]	5.46	3.84	**9.20**	**8.54**
GDINO-T [34]	1.18	1.84	3.94	6.35
GDINO-B [34]	1.97	2.23	6.43	7.58
Shikra [7]	0.80	0.52	2.26	1.60
ONE-PEACE [47]	1.02	0.51	2.64	1.34
SPHINX-v2 [27]	1.59	0.80	4.61	2.36
MiniGPT-v2 [5]	2.69	1.36	6.38	3.29
Ferret [53]	3.18	1.62	8.48	4.43
Kosmos-2 [38]	8.06	4.20	8.64	4.52
Griffon [57]	9.16	4.81	16.77	9.18
Qwen-VL [3]	10.91	5.77	18.32	10.08
CogVLM [50]	**15.38**	**8.33**	**30.73**	**18.15**

Table 4: Experimental results on gRefCOCO [28] dataset. Asterisk (*) denotes results reported in the gRefCOCO paper.

Methods	testA		testB	
	Pr@0.5 ↑	N-acc. ↑	Pr@0.5 ↑	N-acc. ↑
MDETR* [20]	**50.0**	34.5	36.5	31.0
UNINEXT* [52]	46.4	49.3	42.9	48.2
GDINO-T [34]	45.69	79.02	44.83	76.69
NGDINO-T	46.05	**83.17**	**45.57**	**78.08**

Table 5: Experimental results on RSVG [56] dataset. Asterisk (*) denotes results reported in the EarthGPT [58] paper.

Methods	Pr@0.5 ↑	Pr@0.6 ↑	Pr@0.7 ↑	Pr@0.8 ↑
TransVG* [11]	72.41	67.38	60.05	49.10
MGVLF* [56]	76.78	72.68	66.74	56.42
EarthGPT* [58]	76.65	71.93	66.52	56.53
GDINO-T [34]	76.99	75.81	73.36	66.77
NGDINO-T	**77.16**	**76.03**	**73.81**	**67.84**

Our proposed NGDINO consistently outperforms the baseline GDINO [34] across both backbone architectures. Specifically, NGDINO-B achieves state-of-the-art performance, surpassing GDINO-B by significant margins in instance-level metrics (2.48% improvement in F1$_{inst.}$ and 1.77% in Acc$_{inst.}$) as well as image-level metrics (2.32% in F1$_{img.}$ and 1.63% in Acc$_{img.}$).

Zero-shot results. Table 3 presents the zero-shot evaluation results, assessing the models' domain generalization capability. CogVLM [50] demonstrates state-of-the-art performance across metrics. However, several advanced models, including Shikra [7], ONE-PEACE [47], and SPHINX-v2 [27], are limited to outputting only a single bounding box, due to constraints in their pre-training data or output strategy. This restriction significantly impacts their performance in multi-target scenarios.

Additional benchmark evaluations. As presented in Table 4, we evaluate our method on the gRefCOCO [28] benchmark with multi-target and no-target samples. The metric Pr@0.5 measures the percentage of predictions with $F1$ = 1 at IoU $\geq$ 0.5, while N-acc denotes the no-target accuracy. NGDINO-T demonstrates a notable improvement over GDINO-T, especially in the N-acc metric, achieving gains of 4.15% on test A and 1.39% on test B, which assess performance on no-target samples. In contrast, the performance gains in Pr@0.5 (0.36% and 0.74% on test A and B, respectively) are more modest. This can be partially attributed to the relatively simple structure of the multi-target queries in gRefCOCO, where expressions predominantly refer to only one or two objects. MDETR [20] achieves higher Pr@0.5 on the test A set. However, this is likely because MDETR tends to produce more outputs, resulting in lower N-acc performance due to an increased number of false positives on no-target examples.

Table 5 demonstrates our method's effectiveness on the aerial view RSVG [56] benchmark with multi-target samples, where NGDINO-T consistently outperforms previous SOTA methods.

5.2 Ablation studies

Ablation study on NGDINO components. Table 6 presents the analysis of each component in NGDINO. The number prediction head alone shows a slight increase in Acc$_{inst.}$ from 19.02% to

Table 6: Ablation study of NGDINO components on the RefDrone dataset with Swin-Tiny backbone.

Number Prediction Head	Number Cross-Attention	$\mathrm{F1}_{inst.}$	$\mathrm{Acc}_{inst.}$	$\mathrm{F1}_{img.}$	$\mathrm{Acc}_{img.}$	FPS
		30.50	19.02	29.65	21.07	**13.5**
✓		30.62	19.09	29.90	21.18	12.8
	✓	31.25	19.51	30.73	21.71	12.9
✓	✓	**33.34**	**20.98**	**32.45**	**22.84**	12.3

Table 7: Ablation study on the impact of varying selected number query length. Params indicates additional parameters introduced.

Length	$\mathrm{F1}_{inst.}$	$\mathrm{Acc}_{inst.}$	$\mathrm{F1}_{img.}$	$\mathrm{Acc}_{img.}$	Params
1	31.63	19.80	31.23	22.12	**1.58M**
10	**33.34**	**20.98**	**32.45**	**22.84**	1.65M
100	32.06	20.10	32.23	22.81	2.34M

Table 8: Experimental results of two-stage instance ranking methods on the RefDrone benchmark.

Methods	$\mathrm{F1}_{inst.}$	$\mathrm{Acc}_{inst.}$	$\mathrm{F1}_{img.}$	$\mathrm{Acc}_{img.}$
ReCLIP [44]	24.62	14.04	11.58	6.15
GPT4-o	52.38	35.65	35.50	22.38
RDAnnotator	**58.14**	**41.13**	**37.07**	**23.54**

19.09%, indicating the minimal impact of this auxiliary head on REC tasks. When introducing the number cross-attention without number selection, we observe a more substantial improvement, with $\mathrm{Acc}_{inst.}$ increasing to 19.51%. This improvement can be partially attributed to the additional parameters introduced in the decoder. The most significant improvement is achieved through the combination of both the number prediction task and the number cross-attention components. This contribution increases $\mathrm{Acc}_{inst.}$ to 20.98%. While the additional computational cost results in a minor decrease in inference speed (FPS), this trade-off yields a 1.96% increase in $\mathrm{Acc}_{inst.}$.

Ablation study on query length. Table 7 analyzes the impact of varying the selected number query length. Utilizing a minimal query length of 1 lacks the capacity to capture complex numerical information. Conversely, extending the query length to 100 increases parameter count and computational overhead, potentially leading to optimization challenges. Through these experiments, we determine that a query length of 10 provides an optimal trade-off.

Performance on number prediction. The number prediction head achieves an overall number prediction accuracy of 53.5%. During the bounding box prediction stage, this accuracy is observed to be 22.84%. This performance gap demonstrates the effectiveness of the number prediction head. Besides, the number prediction achieves a mean absolute error (MAE) of 0.51, suggesting high precision as predictions closely align with ground truth values.

Performance of two-stage instance ranking method. Table 8 analyzes our annotation framework RDAnnotator (without human verification) against alternative two-stage instance ranking methods for REC tasks. We compare: (1) GPT-4o[2] using only Step 3 of RDAnnotator, and (2) ReCLIP [44], which employs CLIP [40] for instance ranking. All experiments utilize Faster-RCNN [41] as the object detector (18.0 mAP on VisDrone2019-DET [60]). Results show RDAnnotator's ability to produce high-quality annotations. Furthermore, superior instance-level metrics over end-to-end methods reveal the promising potential of two-stage ranking approaches in multi-target challenges.

5.3 Limitations

While NGDINO addresses the multi-target and no-target challenges, several challenges remain. Figure 7 shows some typical NGDINO failure cases, highlighting challenges in RefDrone. The examples show rich contextual reasoning, challenging backgrounds, and small-scale object detection. These challenging cases reflect real applications and highlight areas for future improvement.

6 Conclusion

In this work, we introduce RefDrone, a challenging benchmark specifically designed for referring expression comprehension in drone scenes. The dataset is constructed using the RDAnnotator frame-

[2] https://openai.com/index/hello-gpt-4o/

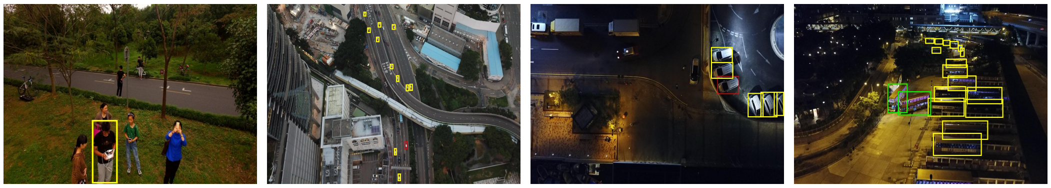

The pedestrian operating a device (possibly a drone controller).

The red cars on the main roads.

The cars parked in a circular pattern near the roundabout.

The buses parked in rows.

Figure 7: Some failure cases of NGDINO on RefDrone dataset. Red, green, and yellow boxes indicate true positives, false positives, and false negatives, respectively.

work, an efficient semi-automated annotation pipeline combining LMM-based modules and human oversight. RDAnnotator provides high-quality annotations while reducing human effort. Furthermore, we develop NGDINO to address the multi-target and no-target challenges in RefDrone. Experimental results demonstrate consistently low performance across existing approaches, underscoring the inherent difficulty of the RefDrone benchmark. In the future, we aim to further enhance NGDINO to address additional challenges presented by RefDrone. We also plan to extend RefDrone to larger-scale scenarios and introduce additional tasks such as referring expression segmentation and referring expression tracking. We believe RefDrone will serve as a valuable benchmark for advancing research in drone-based REC tasks.

References

[1] Telmo Adão, Jonáš Hruška, Luís Pádua, José Bessa, Emanuel Peres, Raul Morais, and Joaquim Joao Sousa. Hyperspectral imaging: A review on uav-based sensors, data processing and applications for agriculture and forestry. *Remote sensing*, 9(11):1110, 2017. 1

[2] Robert L Axtell. Zipf distribution of us firm sizes. *science*, 293(5536):1818–1820, 2001. 7

[3] Jinze Bai, Shuai Bai, Shusheng Yang, Shijie Wang, Sinan Tan, Peng Wang, Junyang Lin, Chang Zhou, and Jingren Zhou. Qwen-VL: A frontier large vision-language model with versatile abilities. *arXiv preprint arXiv:2308.12966*, 2023. 3, 7, 8

[4] Wenzhe Cai, Siyuan Huang, Guangran Cheng, Yuxing Long, Peng Gao, Changyin Sun, and Hao Dong. Bridging zero-shot object navigation and foundation models through pixel-guided navigation skill. In *IEEE Int. Conf. Robot. Autom.*, pages 5228–5234, 2024. 1

[5] Jun Chen, Deyao Zhu, Xiaoqian Shen, Xiang Li, Zechun Liu, Pengchuan Zhang, Raghuraman Krishnamoorthi, Vikas Chandra, Yunyang Xiong, and Mohamed Elhoseiny. MiniGPT-v2: large language model as a unified interface for vision-language multi-task learning. *arXiv preprint arXiv:2310.09478*, 2023. 3, 7, 8

[6] Kai Chen, Jiaqi Wang, Jiangmiao Pang, Yuhang Cao, Yu Xiong, Xiaoxiao Li, Shuyang Sun, Wansen Feng, Ziwei Liu, Jiarui Xu, Zheng Zhang, Dazhi Cheng, Chenchen Zhu, Tianheng Cheng, Qijie Zhao, Buyu Li, Xin Lu, Rui Zhu, Yue Wu, Jifeng Dai, Jingdong Wang, Jianping Shi, Wanli Ouyang, Chen Change Loy, and Dahua Lin. MMDetection: Open mmlab detection toolbox and benchmark. *arXiv preprint arXiv:1906.07155*, 2019. 14

[7] Keqin Chen, Zhao Zhang, Weili Zeng, Richong Zhang, Feng Zhu, and Rui Zhao. Shikra: Unleashing multimodal llm's referential dialogue magic. *arXiv preprint arXiv:2306.15195*, 2023. 3, 7, 8

[8] Yixin Chen, Qing Li, Deqian Kong, Yik Lun Kei, Song-Chun Zhu, Tao Gao, Yixin Zhu, and Siyuan Huang. YouRefIt: Embodied reference understanding with language and gesture. In *Int. Conf. Comput. Vis.*, pages 1385–1395, 2021. 3

[9] Zhenfang Chen, Peng Wang, Lin Ma, Kwan-Yee K Wong, and Qi Wu. Cops-Ref: A new dataset and task on compositional referring expression comprehension. In *IEEE Conf. Comput. Vis. Pattern Recog.*, pages 10086–10095, 2020. 3

[10] Harm De Vries, Florian Strub, Sarath Chandar, Olivier Pietquin, Hugo Larochelle, and Aaron Courville. GuessWhat?! visual object discovery through multi-modal dialogue. In *IEEE Conf. Comput. Vis. Pattern Recog.*, pages 5503–5512, 2017. 3

[11] Jiajun Deng, Zhengyuan Yang, Tianlang Chen, Wengang Zhou, and Houqiang Li. TransVG: End-to-end visual grounding with transformers. In *Int. Conf. Comput. Vis.*, pages 1769–1779, 2021. 8

[12] Yue Fan, Winson Chen, Tongzhou Jiang, Chun Zhou, Yi Zhang, and Xin Wang. Aerial vision-and-dialog navigation. In *Findings of ACL*, pages 3043–3061, 2023. 1

[13] Zhe Gan, Yen-Chun Chen, Linjie Li, Chen Zhu, Yu Cheng, and Jingjing Liu. Large-scale adversarial training for vision-and-language representation learning. *Adv. Neural Inform. Process. Syst.*, 33:6616–6628, 2020. 3

[14] Chen Gao, Baining Zhao, Weichen Zhang, Jun Zhang, Jinzhu Mao, Zhiheng Zheng, Fanhang Man, Jianjie Fang, Zile Zhou, Jinqiang Cui, Xinlei Chen, and Yong Li. EmbodiedCity: A benchmark platform for embodied agent in real-world city environment. *arXiv preprint arXiv:2410.09604*, 2024. 1

[15] Zeyu Han, Fangrui Zhu, Qianru Lao, and Huaizu Jiang. Zero-shot referring expression comprehension via structural similarity between images and captions. In *IEEE Conf. Comput. Vis. Pattern Recog.*, pages 14364–14374, 2024. 3

[16] Richang Hong, Daqing Liu, Xiaoyu Mo, Xiangnan He, and Hanwang Zhang. Learning to compose and reason with language tree structures for visual grounding. *IEEE Trans. Pattern Anal. Mach. Intell.*, 44(2):684–696, 2019. 3

[17] Edward J Hu, Yelong Shen, Phillip Wallis, Zeyuan Allen-Zhu, Yuanzhi Li, Shean Wang, Lu Wang, and Weizhu Chen. LoRA: Low-rank adaptation of large language models. *Int. Conf. Learn. Represent.*, 2022. 14

[18] Ronghang Hu, Marcus Rohrbach, Jacob Andreas, Trevor Darrell, and Kate Saenko. Modeling relationships in referential expressions with compositional modular networks. In *IEEE Conf. Comput. Vis. Pattern Recog.*, pages 1115–1124, 2017. 3

[19] Wei Ji, Li Li, Hao Fei, Xiangyan Liu, Xun Yang, Juncheng Li, and Roger Zimmermann. Towards complex-query referring image segmentation: A novel benchmark. *arXiv preprint arXiv:2309.17205*, 2023. 3, 6

[20] Aishwarya Kamath, Mannat Singh, Yann LeCun, Gabriel Synnaeve, Ishan Misra, and Nicolas Carion. MDETR-modulated detection for end-to-end multi-modal understanding. In *Int. Conf. Comput. Vis.*, pages 1780–1790, 2021. 3, 7, 8

[21] Sahar Kazemzadeh, Vicente Ordonez, Mark Matten, and Tamara Berg. Referitgame: Referring to objects in photographs of natural scenes. In *Proc. EMNLP*, pages 787–798, 2014. 3

[22] Ranjay Krishna, Yuke Zhu, Oliver Groth, Justin Johnson, Kenji Hata, Joshua Kravitz, Stephanie Chen, Yannis Kalantidis, Li-Jia Li, David A Shamma, et al. Visual genome: Connecting language and vision using crowdsourced dense image annotations. *Int. J. Comput. Vis.*, 123:32–73, 2017. 3

[23] Jungdae Lee, Taiki Miyanishi, Shuhei Kurita, Koya Sakamoto, Daichi Azuma, Yutaka Matsuo, and Nakamasa Inoue. CityNav: Language-goal aerial navigation dataset with geographic information. *arXiv preprint arXiv:2406.14240*, 2024. 1

[24] Ke Li, Gang Wan, Gong Cheng, Liqiu Meng, and Junwei Han. Object detection in optical remote sensing images: A survey and a new benchmark. *ISPRS journal of photogrammetry and remote sensing*, 159:296–307, 2020. 3

[25] Liunian Harold Li, Pengchuan Zhang, Haotian Zhang, Jianwei Yang, Chunyuan Li, Yiwu Zhong, Lijuan Wang, Lu Yuan, Lei Zhang, Jenq-Neng Hwang, et al. Grounded language-image pre-training. In *IEEE Conf. Comput. Vis. Pattern Recog.*, pages 10965–10975, 2022. 3, 7, 8

[26] Tsung-Yi Lin, Michael Maire, Serge Belongie, James Hays, Pietro Perona, Deva Ramanan, Piotr Dollár, and C Lawrence Zitnick. Microsoft COCO: Common objects in context. In *Eur. Conf. Comput. Vis.*, pages 740–755, 2014. 3

[27] Ziyi Lin, Chris Liu, Renrui Zhang, Peng Gao, Longtian Qiu, Han Xiao, Han Qiu, Chen Lin, Wenqi Shao, Keqin Chen, et al. SPHINX: The joint mixing of weights, tasks, and visual embeddings for multi-modal large language models. *arXiv preprint arXiv:2311.07575*, 2023. 3, 7, 8

[28] Chang Liu, Henghui Ding, and Xudong Jiang. GRES: Generalized referring expression segmentation. In *IEEE Conf. Comput. Vis. Pattern Recog.*, pages 23592–23601, 2023. 2, 3, 5, 8, 14

[29] Daqing Liu, Hanwang Zhang, Feng Wu, and Zheng-Jun Zha. Learning to assemble neural module tree networks for visual grounding. In *Int. Conf. Comput. Vis.*, pages 4673–4682, 2019. 3

[30] Haotian Liu, Chunyuan Li, Qingyang Wu, and Yong Jae Lee. Visual instruction tuning. *Adv. Neural Inform. Process. Syst.*, 36, 2023. 3, 7, 8

[31] Kehui Liu, Zixin Tang, Dong Wang, Zhigang Wang, Bin Zhao, and Xuelong Li. COHERENT: Collaboration of heterogeneous multi-robot system with large language models. *arXiv preprint arXiv:2409.15146*, 2024. 1

[32] Runtao Liu, Chenxi Liu, Yutong Bai, and Alan L Yuille. CLEVR-Ref+: Diagnosing visual reasoning with referring expressions. In *IEEE Conf. Comput. Vis. Pattern Recog.*, pages 4185–4194, 2019. 3

[33] Shilong Liu, Shijia Huang, Feng Li, Hao Zhang, Yaoyuan Liang, Hang Su, Jun Zhu, and Lei Zhang. DQ-DETR: Dual query detection transformer for phrase extraction and grounding. In *Proc. AAAI Conf. Artif. Intell.*, volume 37, pages 1728–1736, 2023. 3

[34] Shilong Liu, Zhaoyang Zeng, Tianhe Ren, Feng Li, Hao Zhang, Jie Yang, Chunyuan Li, Jianwei Yang, Hang Su, Jun Zhu, et al. Grounding DINO: Marrying dino with grounded pre-training for open-set object detection. *Eur. Conf. Comput. Vis.*, 2024. 2, 3, 6, 7, 8, 14, 16

[35] Shubo Liu, Hongsheng Zhang, Yuankai Qi, Peng Wang, Yanning Zhang, and Qi Wu. AerialVLN: Vision-and-language navigation for uavs. In *Int. Conf. Comput. Vis.*, pages 15384–15394, 2023. 1

[36] Junhua Mao, Jonathan Huang, Alexander Toshev, Oana Camburu, Alan L Yuille, and Kevin Murphy. Generation and comprehension of unambiguous object descriptions. In *IEEE Conf. Comput. Vis. Pattern Recog.*, pages 11–20, 2016. 1, 3, 5

[37] Kunyu Peng, Jia Fu, Kailun Yang, Di Wen, Yufan Chen, Ruiping Liu, Junwei Zheng, Jiaming Zhang, M. Saquib Sarfraz, Rainer Stiefelhagen, and Alina Roitberg. Referring atomic video action recognition. In *Eur. Conf. Comput. Vis.*, 2024. 3

[38] Zhiliang Peng, Wenhui Wang, Li Dong, Yaru Hao, Shaohan Huang, Shuming Ma, Qixiang Ye, and Furu Wei. Grounding multimodal large language models to the world. In *Int. Conf. Learn. Represent.*, 2024. 3, 7, 8

[39] Mengxue Qu, Yu Wu, Wu Liu, Xiaodan Liang, Jingkuan Song, Yao Zhao, and Yunchao Wei. RIO: A benchmark for reasoning intention-oriented objects in open environments. *Adv. Neural Inform. Process. Syst.*, 36, 2023. 3

[40] Alec Radford, Jong Wook Kim, Chris Hallacy, Aditya Ramesh, Gabriel Goh, Sandhini Agarwal, Girish Sastry, Amanda Askell, Pamela Mishkin, Jack Clark, et al. Learning transferable visual models from natural language supervision. In *Int. Conf. Mach. Learn.*, pages 8748–8763, 2021. 9

[41] Shaoqing Ren, Kaiming He, Ross Girshick, and Jian Sun. Faster R-CNN: Towards real-time object detection with region proposal networks. *IEEE Trans. Pattern Anal. Mach. Intell.*, 39(6):1137–1149, 2017. 9

[42] Khin Thida San, Sun Ju Mun, Yeong Hun Choe, and Yoon Seok Chang. Uav delivery monitoring system. In *MATEC Web of Conferences*, volume 151, page 04011, 2018. 1

[43] Qie Sima, Sinan Tan, Huaping Liu, Fuchun Sun, Weifeng Xu, and Ling Fu. Embodied referring expression for manipulation question answering in interactive environment. In *ICRA*, 2023. 1

[44] Sanjay Subramanian, Will Merrill, Trevor Darrell, Matt Gardner, Sameer Singh, and Anna Rohrbach. ReCLIP: A strong zero-shot baseline for referring expression comprehension. In *Proc. ACL*, 2022. 3, 9

[45] Leon Amadeus Varga, Benjamin Kiefer, Martin Messmer, and Andreas Zell. SeaDronesSee: A maritime benchmark for detecting humans in open water. In *Proceedings of the IEEE/CVF winter conference on applications of computer vision*, pages 2260–2270, 2022. 1

[46] Chunlei Wang, Wenquan Feng, Xiangtai Li, Guangliang Cheng, Shuchang Lyu, Binghao Liu, Lijiang Chen, and Qi Zhao. OV-VG: A benchmark for open-vocabulary visual grounding. *Neurocomputing*, 591:127738, 2024. 3

[47] Peng Wang, Shijie Wang, Junyang Lin, Shuai Bai, Xiaohuan Zhou, Jingren Zhou, Xinggang Wang, and Chang Zhou. ONE-PEACE: Exploring one general representation model toward unlimited modalities. *arXiv preprint arXiv:2305.11172*, 2023. 3, 7, 8

[48] Tai Wang, Xiaohan Mao, Chenming Zhu, Runsen Xu, Ruiyuan Lyu, Peisen Li, Xiao Chen, Wenwei Zhang, Kai Chen, Tianfan Xue, et al. Embodiedscan: A holistic multi-modal 3d perception suite towards embodied ai. In *CVPR*, 2024. 1

[49] Tianyu Wang, Haitao Lin, Junqiu Yu, and Yanwei Fu. Polaris: Open-ended interactive robotic manipulation via syn2real visual grounding and large language models. In *International Conference on Intelligent Robots and Systems*, 2024. 1

[50] Weihan Wang, Qingsong Lv, Wenmeng Yu, Wenyi Hong, Ji Qi, Yan Wang, Junhui Ji, Zhuoyi Yang, Lei Zhao, Xixuan Song, et al. CogVLM: Visual expert for pretrained language models. *arXiv preprint arXiv:2311.03079*, 2023. 3, 7, 8

[51] Chi Xie, Zhao Zhang, Yixuan Wu, Feng Zhu, Rui Zhao, and Shuang Liang. Described object detection: Liberating object detection with flexible expressions. *Adv. Neural Inform. Process. Syst.*, 36, 2023. 3

[52] Bin Yan, Yi Jiang, Jiannan Wu, Dong Wang, Ping Luo, Zehuan Yuan, and Huchuan Lu. Universal instance perception as object discovery and retrieval. In *IEEE Conf. Comput. Vis. Pattern Recog.*, pages 15325–15336, 2023. 3, 8

[53] Haoxuan You, Haotian Zhang, Zhe Gan, Xianzhi Du, Bowen Zhang, Zirui Wang, Liangliang Cao, Shih-Fu Chang, and Yinfei Yang. Ferret: Refer and ground anything anywhere at any granularity. *Int. Conf. Learn. Represent.*, 2024. 3, 7, 8

[54] Licheng Yu, Patrick Poirson, Shan Yang, Alexander C Berg, and Tamara L Berg. Modeling context in referring expressions. In *Eur. Conf. Comput. Vis.*, pages 69–85, 2016. 1, 3, 5

[55] Sergey Zagoruyko. Wide residual networks. *arXiv preprint arXiv:1605.07146*, 2016. 4, 15

[56] Yang Zhan, Zhitong Xiong, and Yuan Yuan. RSVG: Exploring data and models for visual grounding on remote sensing data. *IEEE Transactions on Geoscience and Remote Sensing*, 61:1–13, 2023. 2, 3, 6, 8, 14

[57] Yufei Zhan, Yousong Zhu, Zhiyang Chen, Fan Yang, Ming Tang, and Jinqiao Wang. Griffon: Spelling out all object locations at any granularity with large language models. In *Eur. Conf. Comput. Vis.*, pages 405–422, 2024. 3, 7, 8

[58] Wei Zhang, Miaoxin Cai, Tong Zhang, Yin Zhuang, and Xuerui Mao. Earthgpt: A universal multi-modal large language model for multi-sensor image comprehension in remote sensing domain. *IEEE Transactions on Geoscience and Remote Sensing*, 2024. 8

[59] Yiming Zhang, ZeMing Gong, and Angel X Chang. Multi3DRefer: Grounding text description to multiple 3d objects. In *Int. Conf. Comput. Vis.*, pages 15225–15236, 2023. 6

[60] Pengfei Zhu, Longyin Wen, Dawei Du, Xiao Bian, Heng Fan, Qinghua Hu, and Haibin Ling. Detection and tracking meet drones challenge. *IEEE Trans. Pattern Anal. Mach. Intell.*, 44(11):7380–7399, 2021. 3, 4, 5, 9

A Appendix

We provide the following appendices for further analysis:

1. Details of the baseline method. (Appendix A.1)
2. Implementation details. (Appendix A.2)
3. Color attribute analysis of RefDrone. (Appendix A.3)
4. Additional dataset examples. (Appendix A.4)
5. Results with respect to different object scales. (Appendix A.5)
6. Results on RefCOCO/+/g datasets. (Appendix A.6)
7. Visualization results analysis. (Appendix A.7)
8. Prompts and examples in RDAnnotator. (Appendix A.8)

A.1 Details of baseline methods

The details for each baseline method:

- *Specialist models:*
  - **MDETR**: ResNet-101 with BERT-Base,
    pretrained on Flickr30k, RefCOCO/+/g, VG.
  - **GLIP**: Swin-Tiny with BERT-Base,
    pretrained on Objects365.
  - **GDINO-T**: Swin-Tiny with BERT-Base,
    pretrained on Objects365, GoldG, GRIT, V3Det.
  - **GDINO-B**: Swin-Base with BERT-Base,
    pretrained on Objects365, GoldG, V3Det.
- *Large multimodal models:*
  - **Kosmos-2**: 1.6B parameters.
  - **ONE-PEACE**: 4B parameters, visual grounding API.
  - **Shikra**: 7B parameters, delta-v1 version.
  - **MiniGPT-v2**: 7B parameters.
  - **LLaVA**: 7B parameters, v1.5 version.
  - **Qwen-VL**: 7B parameters.
  - **Ferret**: 7B parameters.
  - **CogVLM**: 7B parameters, grounding-specific version.
  - **SPHINX-v2**: 13B parameters.
  - **Griffon**: 13B parameters.

A.2 Implementation details

NGDINO implementation. The NGDINO adopts a two-stage procedure to maintain training stability. First, we pre-train the number prediction head on the RefDrone dataset while initializing other components with GDINO [34] parameters. We then fine-tune the entire model. We also evaluate it on the gRefCOCO [28] dataset, which includes no-target and limited multi-target samples. Additionally, we evaluate it on RSVG [56], an aerial-view dataset with multi-target challenges.

Zero-shot evaluation details. For zero-shot evaluation, we use the original model checkpoints as provided in their respective papers. The implementations and checkpoints for GLIP and GDINO are obtained from MMDetection [6].

Fine-tuning evaluation details. Our fine-tuning protocol maintains consistency across all experiments to ensure a fair comparison. We preserve the original learning strategies while excluding random crop augmentation due to its negative effect on position-sensitive samples. For LMMs, we employ the LoRA [17] fine-tuning strategy and follow the instruction tuning data structures. All fine-tuning experiments are run for 5 epochs using 4 NVIDIA A100 GPUs.

A.3 Details of color categorization.

We design a hybrid color extraction pipeline consisting of two main components: (1) a WideResNet-101 classifier [55] trained on HSV color space-based labels. The color labels are refined via manual validation, ensuring robustness to annotation noise and label ambiguity. (2) An LMM-based color consistency module that validates color predictions through structured prompts. The latter cross-checks the classifier's outputs to mitigate ambiguities caused by illumination variance or partial occlusion.

In the RefDrone dataset, color attributes are present in 69% of expressions. We initially use the HSV color space to define six primary colors: white, black, red, blue, green, and yellow. During the annotation process, RDAnnotator expands the color set by adding six more colors: orange, pink, grey, purple, brown, and silver. The distribution of these color terms across the expressions is illustrated in Figure 8.

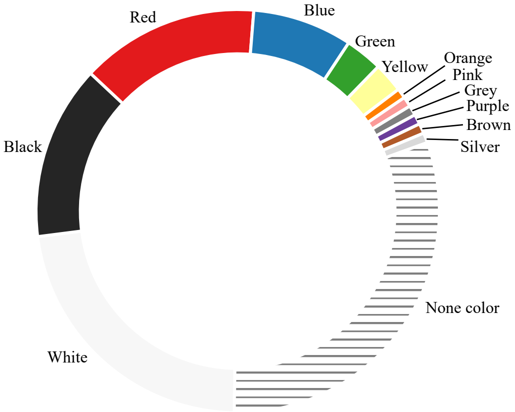

Figure 8: Distribution of color terms in RefDrone expressions.

A.4 Dataset examples

To provide a comprehensive understanding of our RefDrone dataset, we present representative examples in Figure 10. These samples demonstrate the three key challenges in our dataset, highlighting its real-world applicability.

A.5 The results of different object scales.

We add small/medium/large instance accuracy metrics (ACC$_s$, ACC$_m$, ACC$_l$) for the RefDrone dataset in Table 9.

Table 9: Fine-tuned results with respect to different object scales.

Methods	Acc$_s$	Acc$_m$	Acc$_l$	Methods	Acc$_s$	Acc$_m$	Acc$_l$
GLIP	2.65	18.28	27.29	LLaVA	4.18	7.26	11.99
GDINO-T	8.56	20.66	33.99	Qwen-VL	0.73	10.60	30.18
NGDINO-T	**10.84**	**23.38**	**40.13**	RDAnnotator	**32.54**	**47.97**	**47.17**

A.6 Results on RefCOCO/+/g datasets.

Since the RefCOCO, RefCOCO+, RefCOCOg datasets contain only one instance per expression, the proposed NGDINO leverages the number branch primarily to address multi-instance and no-instance scenarios. As a result, the performance of NGDINO is relatively similar to that of GDINO on these datasets.

Table 10: Results on RefCOCO/+/g datasets.

	RefCOCO		RefCOCO+		RefCOCOg	
	TestA	TestB	TestA	TestB	Val	Test
MDETR	90.4	82.67	85.52	72.96	83.35	83.31
GDINO-T	91.4	**86.6**	87.5	74.0	**85.5**	85.8
NGDINO-T	**91.5**	86.5	**87.8**	**74.7**	85.3	**85.8**

A.7 Visualization results compared NGDINO with baseline GDINO.

Figure 9 shows visualization results comparing NGDINO and the baseline GDINO on the proposed RefDrone dataset, demonstrating NGDINO's effectiveness with multi-target samples.

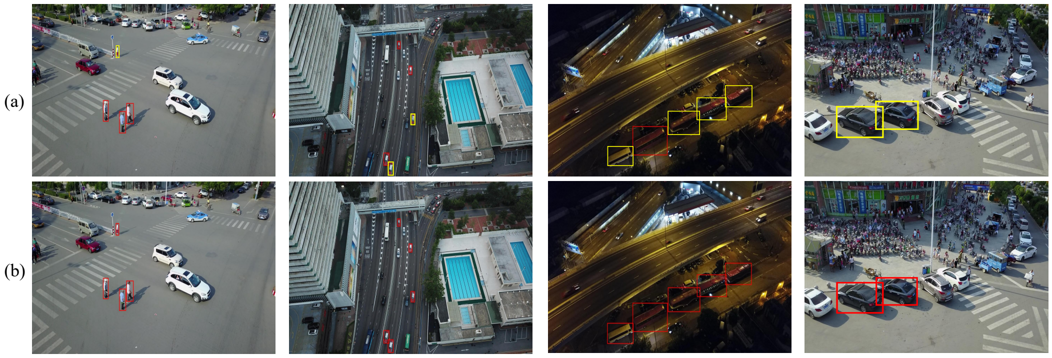

The pedestrians crossing the street.

The red cars driving on the main road.

The buses parked beneath the overpass.

The black cars park in a row on the left side of the image

Figure 9: Visualization results comparing (a) GDINO [34] and (b) NGDINO, where red boxes indicate true positives and yellow boxes denote false negatives.

A.8 Prompts and examples for RDAnnotator

In this section, we provide the prompts and examples employed in RDAnnotator. Table 11 presents the prompt construction process for expression generation (Step 3), which includes the system prompt and few-shot in-context learning examples. One in-context learning example is illustrated in Table 12. The system prompts used for each step are detailed in Table 13. Additionally, the system prompts for the feedback mechanism are presented in Table 14.

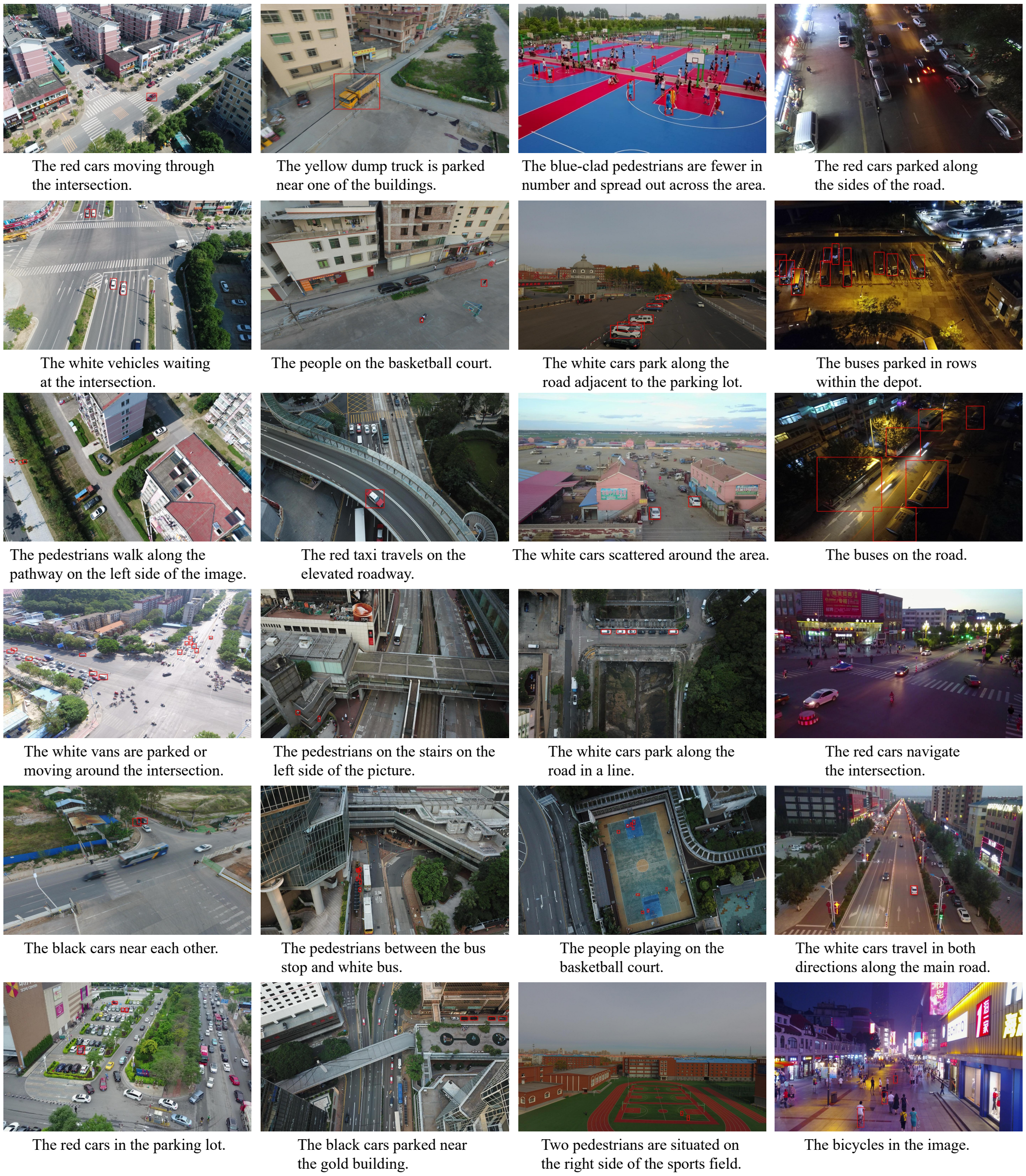

The red cars moving through the intersection.

The yellow dump truck is parked near one of the buildings.

The blue-clad pedestrians are fewer in number and spread out across the area.

The red cars parked along the sides of the road.

The white vehicles waiting at the intersection.

The people on the basketball court.

The white cars park along the road adjacent to the parking lot.

The buses parked in rows within the depot.

The pedestrians walk along the pathway on the left side of the image.

The red taxi travels on the elevated roadway.

The white cars scattered around the area.

The buses on the road.

The white vans are parked or moving around the intersection.

The pedestrians on the stairs on the left side of the picture.

The white cars park along the road in a line.

The red cars navigate the intersection.

The black cars near each other.

The pedestrians between the bus stop and white bus.

The people playing on the basketball court.

The white cars travel in both directions along the main road.

The red cars in the parking lot.

The black cars parked near the gold building.

Two pedestrians are situated on the right side of the sports field.

The bicycles in the image.

Figure 10: Dataset examples from RefDrone.

Table 11: Illustration of RDAnnotator's prompt construction for expression generation (Step 3). Few-shot in-context-learning examples are from `fewshot_samples`. A representative example is shown in Table 12

```
messages = [ {"role":"system", "content": f"""As an AI visual assistant, your role involves
analyzing a single image. You are supplied with three sentences that caption the image, along with
additional data about specific attributes of objects within the image. This can include information
about categories, colors, and precise coordinates. Such coordinates, represented as floating-point
numbers that range from 0 to 1, are shared as center points, denoted as (x, y), identifying the center x
and y. When coordinate x tends to 0, the object nears the left side of the image, shifting towards the
right as coordinate x approaches 1. When coordinate y tends to 0, the object nears the top of the
image, shifting towards the bottom as coordinate y approaches 1.

Your task is to classify the provided objects based on various characteristics, while also substantiating
your classification. This classification should be thoroughly justified, with criteria including but not
limited to relationships or relative locations of objects.

To refer to a specific object, use the provided coordinates directly. Base your classification justifica-
tions on direct observations from the image, avoiding any hypothesizing or assumptions."""}
]
for sample in fewshot_samples messages.append({"role":"user",
"content":sample[‘context’]})
messages.append({"role":"assistant", "content":sample[‘response’]} )
messages.append({"role":"user", "content":‘\n’.join(query)})
```

Table 12: One example to illustrate the input and output in RDAnnotator Step 3 (expression generation). The top block shows the input contexts such as image, object, caption and color attributed. The bottom block shows the generated annotations.

Context type 1: Captions

The image shows an aerial view of a busy urban street with multiple lanes of traffic, flanked by parking areas and buildings. A median strip with greenery runs down the center, dividing the opposite flows of vehicles. On either side of the road, there are commercial and residential structures. Parking lanes on both sides of the main road are filled with parked vehicles.
The image shows a bird's-eye view of an urban street scene with traffic congestion...⟨omitted⟩

Context type 2: Objects

pedestrian, white: [0.173, 0.849]
car, black: [0.214, 0.975]
car, white: [0.215, 0.904]
car, white: [0.313, 0.444]
car, red: [0.315, 0.256]
van, white: ...⟨omitted⟩

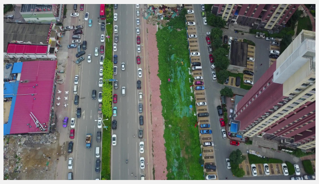

Context type 3: Image

Response :

The blue cars park on the right parking lot.
Coordinates: [0.628, 0.478], [0.646, 0.692], [0.649, 0.727]
The white cars park on both sides of the main road in a line.
Coordinates: [0.431, 0.051], [0.431, 0.15], [0.431, 0.101], [0.434, 0.256], [0.439, 0.523], [0.443, 0.813], [0.445, 0.902], [0.446, 0.982], [0.235, 0.43], [0.232, 0.486], [0.223, 0.674], [0.215, 0.904]

Table 13: System prompts employed at different stages of RDAnnotator, replacing the default system messages shown in Table 11

System prompt: Step 1 scene understanding
You are an AI visual assistant that specializes in providing clear and accurate descriptions of images without any ambiguity or uncertainty. Your descriptions should focus solely on the content of the image itself and avoid mentioning any location-specific details such as regions or countries where the image might have been captured.

System prompt: Step 2 color categorization
As an AI visual assistant, your role involves analyzing a single image.
You are supplied with the specific attributes of objects within the image. This can include information about categories, colors, and precise coordinates. Such coordinates, represented as floating-point numbers that range from 0 to 1, are shared as center points, denoted as (x, y), identifying the center x and y.
Your task is to assess whether the given colors of specific objects match their appearance in the image. Respond with "Yes" when the colors are appropriate. In cases where the colors are deemed inappropriate, respond with a concise "No."

System prompt: Step 3 expression generation
As an AI visual assistant, your role involves analyzing a single image. You are supplied with three sentences that caption the image, along with additional data about specific attributes of objects within the image. This can include information about categories, colors, and precise coordinates. Such coordinates, represented as floating-point numbers that range from 0 to 1, are shared as center points, denoted as (x, y), identifying the center x and y. When coordinate x tends to 0, the object nears the left side of the image, shifting towards the right as coordinate x approaches 1. When coordinate y tends to 0, the object nears the top of the image, shifting towards the bottom as coordinate y approaches 1.
Your task is to classify the provided objects based on various characteristics, while also substantiating your classification. This classification should be thoroughly justified, with criteria including but not limited to relationships or relative locations of objects.
To refer to a specific object, use the provided coordinates directly. Base your classification justifications on direct observations from the image, avoiding any hypothesizing or assumptions.

System prompt: Step 4 quality evaluation
As an AI visual assistant, your role involves analyzing a single image. You are supplied with three sentences that describe the image, along with additional data about specific attributes of objects within the image. This can include information about categories, colors, and precise coordinates. Such coordinates, represented as floating-point numbers that range from 0 to 1, are shared as center points, denoted as (x, y), identifying the center x and y. When coordinate x tends to 0, the object nears the left side of the image, shifting towards the right as coordinate x approaches 1. When coordinate y tends to 0, the object nears the top of the image, shifting towards the bottom as coordinate y approaches 1.
Besides, you are supplied with the description of the objects and their corresponding attributes.
Your task is to confirm whether the description exclusively relates to the described objects without including any others in the visual. Respond "yes" if it matches, or "no" with an explanation if it does not.

Table 14: RDAnnotator system prompts for feedback mechanism. Differences from Table 13 are **highlighted**

System prompt: Step 2 color categorization with feedback mechanism
As an AI visual assistant, your role involves analyzing a single image.
You are supplied with the specific attributes of objects within the image. This can include information about categories, colors, and precise coordinates. Such coordinates, represented as floating-point numbers that range from 0 to 1, are shared as center points, denoted as (x, y), identifying the center x and y.
Your task is to assess whether the given colors of specific objects match their appearance in the image. Respond with "Yes" when the colors are appropriate. In cases where the colors are deemed inappropriate, respond with a concise "No."

System prompt: Step 3 expression generation with feedback mechanism
As an AI visual assistant, your role involves analyzing a single image. You are supplied with three sentences that caption the image, along with additional data about specific attributes of objects within the image. This can include information about categories, colors, and precise coordinates. Such coordinates, represented as floating-point numbers that range from 0 to 1, are shared as center points, denoted as (x, y), identifying the center x and y. When coordinate x tends to 0, the object nears the left side of the image, shifting towards the right as coordinate x approaches 1. When coordinate y tends to 0, the object nears the top of the image, shifting towards the bottom as coordinate y approaches 1.
You are also provided with descriptions and the objects that initially failed to match, along with the reasons for the discrepancies.
Your task is to revise both the description and the corresponding objects to correct these mismatches based on the provided reasons. Ensure that the revised description accurately matches the corresponding objects depicted in the visual content.

System prompt: Step 4 quality evaluation with feedback mechanism
As an AI visual assistant, your role involves analyzing a single image. You are supplied with three sentences that describe the image, along with additional data about specific attributes of objects within the image. This can include information about categories, colors, and precise coordinates. Such coordinates, represented as floating-point numbers that range from 0 to 1, are shared as center points, denoted as (x, y), identifying the center x and y. When coordinate x tends to 0, the object nears the left side of the image, shifting towards the right as coordinate x approaches 1. When coordinate y tends to 0, the object nears the top of the image, shifting towards the bottom as coordinate y approaches 1.
Besides, you are supplied with the description and the objects that initially failed to match.
Your task is to provide detailed reasoning for unsuccessful object matches.